DOI: 10.1007/s12541-012-0227-8

Efficient Workpiece Clamping by Indenting Cone-shaped Elements

Branko Tadic[1], Branislav Jeremic[1], Petar Todorovic[1], Djordje Vukelic[2,#], Uros Proso[1], Vesna Mandic[1], and Igor Budak[2]

1 Department for Production Engineering, Faculty of Engineering, University of Kragujevac, Sestre Janjic 6, Kragujevac, Serbia, 34 000
2 Department for Production Engineering, Faculty of Technical Sciences, University of Novi Sad, Trg Dositeja Obradovica 6, Novi Sad, Serbia, 21 000
Corresponding Author / E-mail: vukelic@uns.ac.rs, TEL: +381-21-485-2326, FAX: +381-21-454-495

KEYWORDS: Clamping, Compliance, Indenting, Load capacity, Fixture

Machining fixtures which utilize screw-or strap clamps are widely used in manufacturing. Typical for them is that the cutting forces are balanced by the friction forces which act on the contact surfaces (interfaces) between clamping elements (screw- or strap clamps) and workpiece. This paper analyses load capacity and compliance of these interfaces. In order to increase their load capacity and reduce compliance, a method is proposed which is based on indenting sharp cone-shaped clamping elements into workpiece material using appropriate surfaces which are not machined, and are not expected to satisfy any particular aesthetic demands (most often castings and forgings). The results of numerical simulations and experimental investigation reveal substantial advantages of the proposed clamping method, offering possibility for industrial application and further investigation.

Manuscript received: December 26, 2011 / Accepted: May 1, 2012

1. Introduction

With the recent rapid development of industry, the need has increased for precision cutting of various kinds of machine parts. In particular, in the cutting industry, it is important to enhance cutting efficiency and precision simultaneously.[1] Within a manufacturing system, there are several factors which most prominently influence the quality of process plans: blanks, sequence and structure of machining processes, concentration of machining operations, machine tools, cutting tools, fixtures, measuring devices, etc. Enhancement of process planning procedure requires optimization of these parameters.[2]

The demand to manufacture low cost products with better quality has forced the manufacturing industry to continuously progress in machining technologies.[3] In the chain of factors which influence the quality of final product, fixtures are of exquisite importance. Machining fixture is a precision device used to locate and hold a workpiece firmly in the proper position during manufacturing operations.[4] The design of a fixture is a highly complex and intuitive process, which requires knowledge and experience. Fixtures have direct impact upon product quality, productivity and cost. The costs associated with fixture planning, design and manufacture can account for 10-20% of the total cost of a manufacturing system.[5] This influenced emergence of a number of methodologies aimed at providing fixture layout optimization. Numerous researchers have been focused on the influence of workpiece-fixture system on the total machining accuracy. In that respect, two basic methods can be distinguished:[6]

- configuration optimization of fixture elements and optimization of clamping forces, and
- prediction of workpiece displacement due to the effect of geometric errors and deformation of the workpiece-fixture system.

Deformation analysis has been a key problem in the past decade and has been studied extensively. Within the analysis of workpiece deformations attention has mostly been focused on: kinematic analysis, force analysis, finite-element analysis (FEA), contact analysis, etc. Deformation analysis pertains to the study of local and total deformation.

Amaral et al.[7] used ANSYS parametric design language code to verify fixture design integrity. They employed 3-2-1 locating method and developed an algorithm to automatically optimize fixture support, clamp locations, and clamping forces, to minimize workpiece deformation, subsequently increasing machining accuracy. Asante[8] presented a model that combines contact

elasticity with finite element methods (FEM) to predict contact loads and pressure distribution at the contact region in a workpiece-fixture system. Chen et al.[9] presented a fixture layout design and clamping force optimization procedure based on the genetic algorithm (GA) and FEA. The optimization procedure is multi-objective: minimizing the maximum deformation of the machined surfaces and maximizing the uniformity of the deformation. DeMeter et al.[10] developed a linear programming model to predict the minimum clamp forces for workholding that considers deformation of workpiece and fixture. Their experimental results emphasized the significance of fixture elasticity on workpiece-fixture response to machining load. Hamedi[11] discussed a hybrid learning system that used nonlinear FEA with a supportive combination of artificial neural network and GA. This leads to finding the optimal set of clamping forces that result in a secured workpiece with minimal deformation and stress. Hockenberger and De Meter[12] reported a fixture-workpiece system model for prediction of rigid body displacements of the workpiece during machining. They use empirical contact force displacement relationships (called "meta-functions") to account for the workpiece/fixture elasticity. Huang and Wang[13] minimized the static elastic deformation of the workpiece by varying the clamping force. Kashyap and DeVries[14] used the FEA method to determine positions of the fixture supporting points in order to minimize normal deformations of the workpiece at the primary locating surface. Kaya[15] presented a GA-based continuous fixture layout optimization method. The optimization objective was to search for a 2-D fixture layout that minimizes the maximum elastic deformation at different workpiece locations. Krishnakumar and Melkote[16] presented a GA-based discrete fixture layout optimization method to minimize workpiece deformation under static conditions. They applied GA for 2-D fixturing problems. Krishnakumar et al.[17] presented an iterative algorithm that minimized workpiece elastic deformation for the entire cutting process by alternatively varying the fixture layout and clamping force. Liao et al.[18] developed an finite element (FE) model using surface-to-surface contact elements to model the fixture/workpiece contact. Nonlinear programming technique was used to optimize fixture layout. Liu et al.[19] proposed a method to optimize the fixture layout in the peripheral milling of a low-rigidity workpiece. This paper dealt with the optimization of the number and positions of locators only on the secondary locating surface. Lu et al.[20] created a model of clamping force determination as a multimodal function with a set of geometric and performance constraints. They appled a cellular GA to solve the problem of global optimal clamping forces. Prabhaharan et al.[21] presented a fixture layout optimization method that used GA and ant colony algorithm (ACA) separately. Workpiece deformation was modeled using FEM for the problems of fixture layout optimization with the objective of minimizing the dimensional and form errors. Padmanaban et al.[22] used an ACA-based discrete optimization method to optimize fixture layout under dynamic conditions. They also proved that in the fixture layout optimization ACA out performed GA. Padmanaban et al.[23] optimized fixture layout for 2D workpiece geometry with an objective of minimizing the workpiece elastic deformation using ACA-based discrete and continuous fixture layout optimization methods. Ratchev et al.[24] presented simulation methodology that is capable of predicting the dynamic behaviour of fixture–workpiece systems. Representing workpiece-fixture contacts as spring and/or damper elements, they produced required spring profiles for a range of fixture and workpiece contact scenarios. Sanchez et al.[25] calculated the contact load distribution and valid clamping regions in machining processes. They also calculated the contact load using a non-iterative means by modeling both fixture and workpiece as separate and independent FEM problems. Satyanarayana and Melkote[26] presented a systematic analysis of the FE representation of a fixture–workpiece pair and analyzed the effectiveness of representation of the fixture element using gap element, spring element and surface-to-surface element regarding analytic analysis and experimental results. Sayeed and DeMeter[27] presented a linear, mixed-integer programming model for determination of the optimal fixture layout to reduce the effect of the workpiece static deformation on the geometric error of the machined features. Tan et al.[28] employed available optimization methods to address the clamping location and clamping force optimization problem. The developed model is able to determine in detail the reaction forces, workpiece displacement, deformation in the workpiece and fixtures. In addition, the developed FEM includes fixture stiffness, making a step forward in comparison with previous models which assumed fixtures to be rigid bodies. Vishnupriyan et al.[29] optimized the fixture layout in order to minimize the machining error considering both geometric error of locating elements and elastic deformation of workpiece. Both of these parameters were simultaneously optimized using a GA. Elastic deformation of workpiece under machining loads was obtained by FEM analysis. Wang et al.[30] proposed a method of FE simulation of the fixture–workpiece pair during locating, clamping and machining using a fixture and components. Important factors that impact the FEA prediction accuracy, e.g. component simplification, mesh generation, contact modeling parameters, boundary conditions and load sequence, are considered. Wang et al.[31] proposed a system based on FEA which compares the deformation induced by machining forces to the tolerance. System can mesh workpiece (straight thin-walled cylinder, conic thin-walled cylinder and angle-varying thin-walled cylinder), assign material properties and boundary conditions, and create FEA files ready for calculation with limited human interference. Xiong et al.[32] focused on determination of an optimal clamping scheme, including the magnitudes and positions of clamping forces. They modeled the contacts between workpiece and fixture locators/clamps as locally elastic contacts with friction. The optimization goal is to minimize elastic deformations at workpiece-fixture contacts. Zuperl et al.[33] developed an intelligent fixturing system, which adaptively adjusts variable clamping forces to achieve minimum elastic deformation of the workpiece according to cutter position and cutting forces. The proposed system is characterized by on-line monitoring, dynamic clamping forces, and real-time fixturing process control.

Analysis of previous research leads to several conclusions. Inadequate fixturing process can result in elastic or plastic

workpiece deformations, as well as the displacements which can significantly impact the final workpiece accuracy. On the other hand, insufficient clamping force can cause displacement of workpiece and its detachment from locating elements during machining, rendering the fixturing process inefficient. Deformations and distortions can be minimized by optimization of locating scheme (the number, type, and arrangement of locating elements) and clamping scheme (the number, type, and arrangement of clamping elements, and clamping force intensities), especially in the case of thin-walled and complex-geometry workpieces. Fixture layout optimization is becoming more important bearing in mind that modern manufacturing often requires fixtures which are able to provide stable locating and clamping of very complex workpieces, while the machining is performed with a large number of tools, in various cutting zones, with various cutting regimes and irregular chip cross sections along tool path. Adequate clamping force (which keeps workpiece displacements during machining within tolerances) is often variable and changes its value as the function of tool path and cutting regime parameters, even when machining is performed with a single cutting tool.

Analysis of deformations is used to determine elastic workpiece deformations under the sum of forces (cutting forces, clamping forces, support reactions, gravity force, friction) which directly impact final workpiece dimensions, form and surface quality. The goal of optimization is to find such fixture configuration that minimizes workpiece elastic deformations and deformations due to workpiece contact with fixture elements during entire machining process.

In contrast with the previous investigations, this paper proposes an approach to workpiece clamping based on intentional plastic deformation of workpiece in some predefined narrow zones. This is based on the fact that there are a large number of castings and forgings in industrial practice which, considering their role as a component within assembly, can be plastically deformed within some narrow zones for the purpose of more efficient clamping (greater load capacity and lower compliance at workpiece/fixture interfaces). With this in mind, numerous FEM analyses were performed accompanied by an extensive experimental investigation using a specially designed device. The results obtained indicate that the proposed approach to workpiece clamping has significant advantages over previous methods.

2. Theoretical background of the proposed clamping method and FEM analysis

It is common knowledge that, in many cases, cutting forces are balanced by friction forces between clamping elements and workpiece (Fig. 1).

Within the contact zones (C_1 and C_2) between clamping elements and workpiece, as well as within the contact zones between the workpiece, and fixture locating elements, under the influence of clamping and cutting force F_y, a complex stress state occurs. Cutting force, F_y, causes displacements in the aforementioned

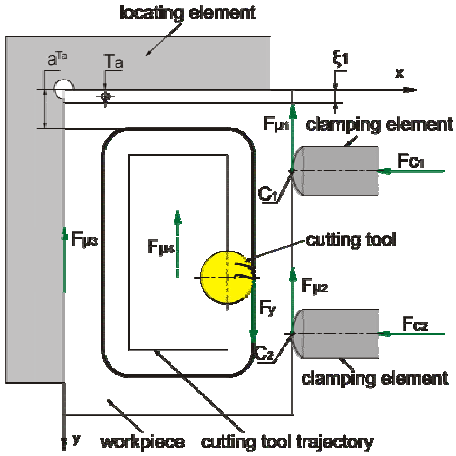

Fig. 1 An example of balancing the cutting forces with forces of friction

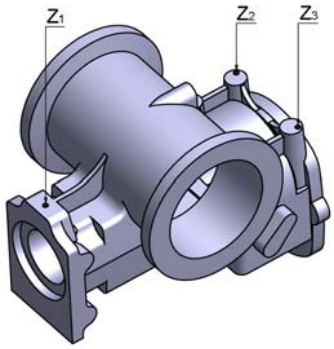

Fig. 2 An example of a casting which can tolerate plastic deformation within the clamping zones, considering its basic function and aesthetic requirements

contact zones, which are described as compliance in the sense and direction of F_y vector. The magnitude of displacements (compliance expressed as coordinate ξ_1) depends on friction force components $F_{\mu 1}$, $F_{\mu 2}$, $F_{\mu 3}$, and $F_{\mu 4}$. The magnitude of workpiece displacements during machining is the result of compliance in the contact zone between the clamping element and workpiece on the one side, and compliance between the workpiece and fixture locating elements. In principle, it depends on the contact load magnitude, i.e., force F_y, and can cause machining error despite the fact that, on the macro-level, the system maintains its static or dynamic stability. That will happen when the magnitude of compliance, ξ_1, oversteps the allowed tolerance of dimension a, i.e., when $\xi_1 \geq T_a$.

Machining accuracy and maximum cutting force, do not depend solely on the clamping forces (F_{C1} and F_{C2}), friction coefficient and friction forces, but also on the macro-geometry of contacts. This macro-geometry defines stress fields distribution and displacements within the contact zones, i.e., their compliance and load capacity.

The clamping method proposed in this paper is based on the fact that there exist a large number of workpieces which require machining of a smaller number of surfaces. The rest of them are not machined since they are neither considered functional, nor have to look aesthetically pleasing. This is most often true for various types of housings, supports, carriers, and similar parts which are manufactured as castings and forgings (Fig. 2).

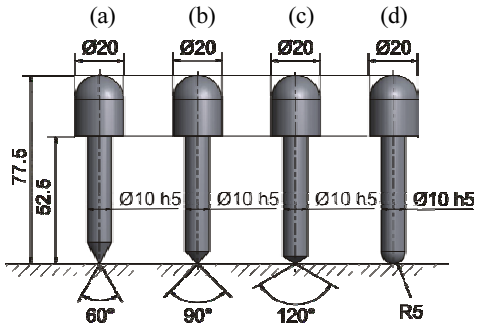

Fig. 3 Geometries of indenters, (a) cone-tip indenter α=60°, (b) cone-tip indenter α=90°, (c) cone tip indenter α=120°, and (d) spherical-tip indenter R=5

The basic function of such parts is not compromised if they are permanently locally deformed within narrow zones. Fig. 2 shows and example of local deformations on a multiplicator housing within zones Z_1, Z_2, and Z_3.

With this in mind, following assumptions are made:

- besides the micro-geometry of contact surfaces, the compliance of interface in the zones where the workpiece is clamped largely depends on the macro-geometry of clamping elements and workpiece,
- the tangential load capacity of interface (in the direction orthogonal to the cutting force) within the clamping zones, also significantly depends on the macro-geometry of contact zones of clamping elements and workpiece, and
- adequate selection of contact zone geometry can significantly increase the load capacity of the clamping element/workpiece interface and reduce its compliance, which positively affects machining accuracy, and allows higher productivity through more stringent cutting regimes.

Therefore, the plan is to perform experimental measurements and numerical simulations to determine the tangential load capacities and compliances of clamping element/workpiece interfaces for four different geometries of clamping elements. The clamping force shall be varied within broad limits. The geometries of clamping elements used in experiments are three cone-tip indenters with various tip angles, and a standard spherical-tip indenter (Fig. 3).

Shown in Fig. 4 is a CAD model with workpiece (1), indenter (2) which applies force F_{ind} to simulate clamping force, F_C, thruster (3) which applies force F_r to simulate cutting force, and base support (4). FEM analyses were performed using Simufact Forming v9.

In the first step, the indenter (2) penetrates the workpiece assuming the pre-defined depth. After this, the indenter makes no motion, whatsoever. The used FEM software allows the indenting force, F_{ind}, to be calculated based on the known depth of indent (obtained experimentally). In the second step (upon completion of indenting process), the workpiece is pushed by the thruster (3) along X axis, while the dependence of thrust force F_r on the thruster travel is monitored and recorded. The friction between the immovable base support (4) and workpiece (1) is disregarded,

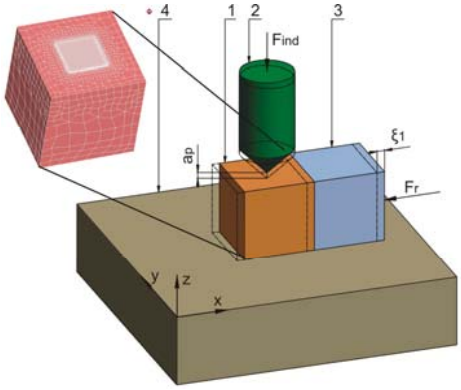

Fig. 4 CAD model of workpiece, indenter, thruster, and base support

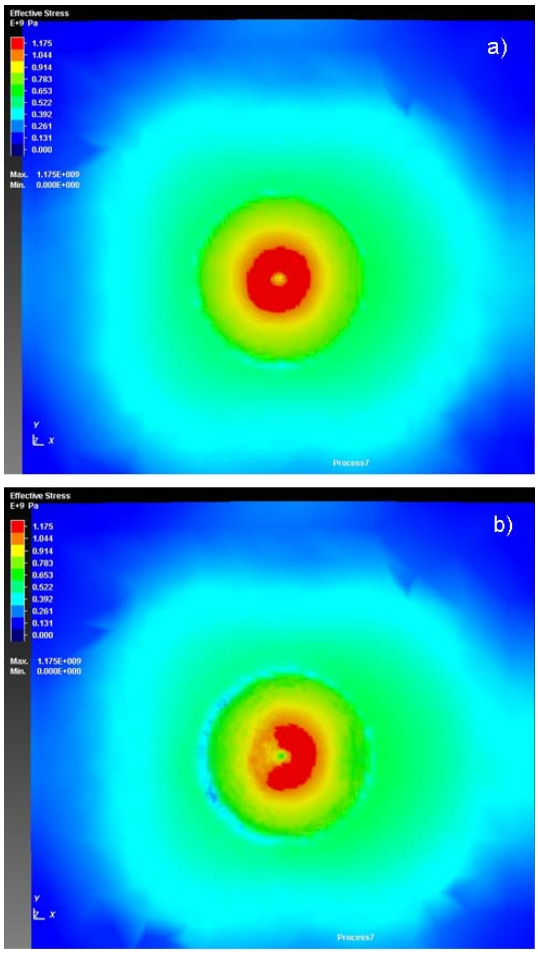

Fig. 5 Stress field distribution in the contact zone, (a) after indenting cone-tip indenter α=90° at the depth of a_p=1.621mm (b) after full thrust

bearing in mind that the objective is to examine just the compliance, ξ_1, between the indenter (2) and workpiece (1). Beside the depth of indent, a_p, the input parameters for FEM analysis were following:

- Flow stress-strain curve, which, for the workpiece material C 45 E, has the following form:

$$\sigma = 367.37 + 599.96 \cdot \varepsilon^{0.3433} \text{ [MPa]} \quad (1)$$

- Dependence between stress, σ, and relative deformation, ε, in equation (1) is given by correlation coefficient, R = 0.998.

Table 1 Regression equations and correlation coefficients, R, obtained by statistical analysis of FEM output results

Indenter	Regression equation	R
Cone α=60°	$F_r = -7549.69 \cdot \xi_1 - 0.038408 \cdot F_{ind} - 224.794 \cdot \xi_1^{2900.793} + 120.6099 \cdot (\xi_1 \cdot F_{ind})^{1/2}$	0.976
Cone α=90°	$F_r = -6800.32 \cdot \xi_1 - 0.019892 \cdot F_{ind} - 1106.59 \cdot \xi_1^{403.1061} + 92.43569 \cdot (\xi_1 \cdot F_{ind})^{1/2}$	0.980
Cone α=120°	$F_r = -9.29830 \cdot \xi_1 - 0.038149 \cdot F_{ind} - 227.228 \cdot \xi_1^{0.0735591} + 70.74752 \cdot (\xi_1 \cdot F_{ind})^{1/2}$	0.991
Speherical R=5	$F_r = -4444.95 \cdot \xi_1 + 0.008408 \cdot F_{ind} - 15.2560 \cdot \xi_1^{-0.442781} + 75.06031 \cdot (\xi_1 \cdot F_{ind})^{1/2}$	0.988

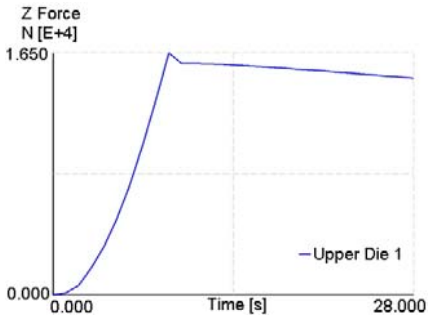

Fig. 6 Time dependence of indenting force Find on time - data obtained for cone-tip indenter α=90° at the depth of a_p=1.621mm

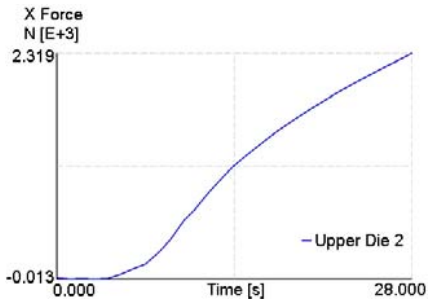

Fig. 7 Time dependence of interface load capacity in the direction of simulated cutting force, F_r - data obtained for cone-tip indenter α=90° at the depth of a_p=1.621mm

- Coefficient of friction between the indenters and test inserts, μ=0.15, was determined by tribometer tests (indenters - tool steel, HS 18-0-1, hardness 64HRC, test inserts - steel C 45 E).
- Mesh parameters (Fig. 4) - 7300 hexahedral elements, 1.5mm size, the contact zone area significantly refined (0.09375mm element size).
- Indenting speed - 0.1mm/s.

In order to create identical conditions for the comparison of numerical simulation and experimental results, calculations were made for all of the four indenter geometries (Fig. 3) and depths of indent, obtained experimentally, with following indenting forces, F_{ind}: 400N, 640N, 1800N, 2900N, 4500N, 5700N, 7000N, 9000N, 11000N, and 13000N. For example, using the cone-tip indenter α=90°, following depths of indent, a_p, were simulated: 0.246mm, 0.340mm, 0.6015mm, 0.786mm, 0.966mm, 1.094mm, 1.298mm, 1.432mm, and 1.621mm. Using these input data, *10x4*=40 different simulations of the process were performed, thus providing a critical mass of data for statistical analysis.

Fig. 5(a) shows stress fields distribution in the contact area, obtained by FEM analysis for cone-tip indenter α=90°, and indent depth a_p=1.621mm. Fig. 5(b) shows stress fields distribution upon the thruster applied pressure. In addition, Fig. 6 shows the change

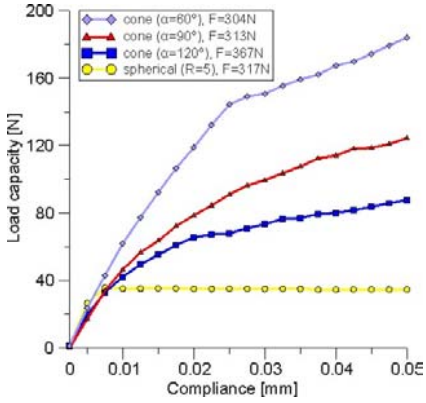

Fig. 8 Dependence of interface load capacity, F_r, on interface compliance, ξ_1, obtained for all four indenter geometries at relatively small indenting forces

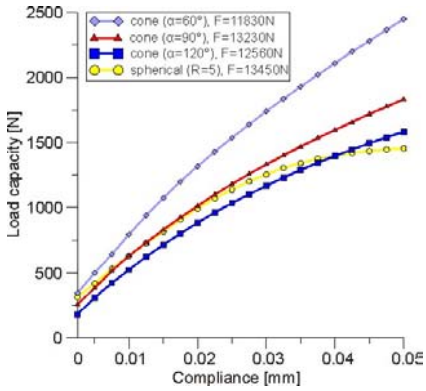

Fig. 9 Dependence of interface load capacity, F_r, on interface compliance, ξ_1, obtained for all four indenter geometries at relatively large indenting forces

of indenting force with time, while Fig. 7 illustrates the change of axial interface load capacity with time, i.e., thrust travel. Obviously, the magnitude of thrust travel corresponds to the axial force causing the movement. The thrust travel corresponds to interface compliance, while the magnitude of force acting on the thruster equals the interface load capacity.

Statistical analysis of a large number of FEM output results, yielded regression equations which best describe the dependence of interface load capacity, F_r, on interface compliance, ξ_1, and indenting force, F_{ind}, for all four indenter geometries. A non-linear regression analysis was performed in Statistica 8, using the simplex method. The regression equations and their corresponding coefficients of correlation, R, are presented in Table 1.

Shown in Figs. 8 and 9 are the dependencies of interface load capacity, F_r, on interface compliance, ξ_1, obtained by numerical simulation, with all four indenter geometries, and depths of indent, a_p. Tha data in Figs. 8 and 9 correspond to indenting forces F_{ind} =

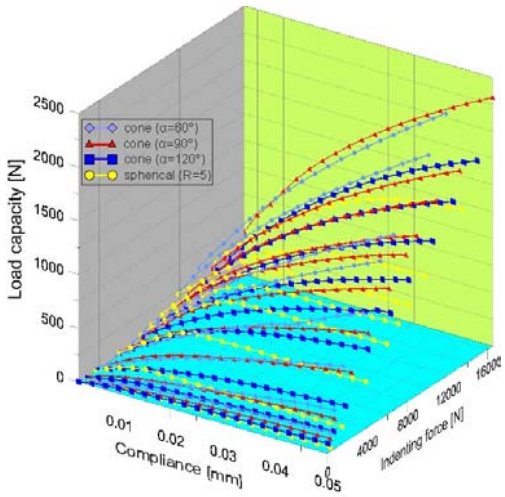

Fig. 10 3D diagram of dependence of interface load capacity, F_r, on interface compliance, ξ_1, indenting force, F_{ind}, and indenter geometry

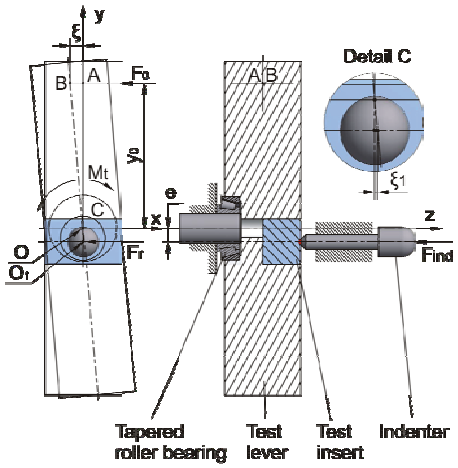

Fig. 11 Principle diagram of the device for measurement of interface load capacity and compliance

400N (Fig. 13) and F_{ind}=13000N (Fig. 14), obtained experimentally.

Shown in Fig. 10 is a 3D diagram of FEM analysis results illustrating the dependence of interface load capacity, F_r, on interface compliance, ξ_1, indenting force, F_{ind}, and indenter geometry.

Considering the interface compliance (Fig. 8), all cone-tip indenters are better than the spherical-tip one in the domain of lower loads and compliances greater than 0.0075 mm. Numerical results shown in Fig. 9 also indicate superiority of 60° and 90° cone-tip indenters (α=60°, α=90°) in the domain of larger indenting forces, where they allow higher interface compliance. The 3D diagram in Fig. 10 - obtained through numerical simulations for four indenter geometries and ten indenting forces - also shows that cone-tip indenters allow higher load capacities compared to spherical-tip indenter.

3. Experimental investigation

Experimental investigations included measurement of load capacity, F_r, and interface compliance, ξ_1 (the interface between the indenter and test inserts) which transfers the load (force or torque) onto the workpiece, causing stress fields within the contact zone. The experiment included:

- variation of indenting force, F_{ind}, within interval of 400N to 13000N,
- variation of indenter/test insert interface load capacity, F_r, within the 5N to 2500N interval, and
- monitoring of interface compliance, ξ_1, expressed as displacement within the contact zone.

Following instrumentation was used during experiment:

- Specially designed and manufactured device, shown as a diagram in Fig. 11, and photographed in Fig. 12. The device functions on mechanical principle, using lever mechanisms and calibrated weights. It allows the indenters to be pressed into test inserts by an exact indenting force, F_{ind}, in order to simulate loads on the indenter/test insert interface, F_r, and monitor interface compliance, ξ_1.
- Comparators-indicators of displacement with accuracy of 0.01mm, which increase accuracy of measurement by showing displacement 22.5 times greater than the real displacements within the indenter/test insert contact zone. Using geometric parameters shown in Fig. 11, the readings are transformed into real displacements.
- Once the indenter/test insert assembly was disassembled, the measurement of diameters of indented profiles on the surface of test inserts was performed using a high-resolution (4800dpi) scanner and image processing in ZEISS AxioVision software.

Test lever is supported by a tapered roller bearing in *X*-axis which passes through the center of gravity (Fig. 11). This bearing allows the test lever to be rotated about point *O*, in *X*-*Y* plane. Test insert, which is attached to the test lever, is indented by the indenters of predefined geometries (Fig. 3). Indenting is performed at point O_1 which is offset in the *Y* direction, by *e*, relative to rotation axis of the test lever. The various magnitudes of indenting force, F_{ind}, are provided by a specially designed lever mechanism and calibrated weights. Once the indenter has penetrated the test insert, force F_o is applied to the test lever at point *A*, at distance y_o from the fulcrum, and the resulting displacement, ξ, is monitored. The F_o is incremented from minimum to maximum value. In this way, a series of corresponding F_o- ξ value pairs was obtained for each combination of indenter geometry and simulated indenting force, F_{ind}. It is obvious that the indenting force, F_{ind}, simulates the clamping force, F_o simulates tangential load capacity of the test insert/indenter interface, while the displacement ξ represents interface compliance at point *A*.

Based on geometric relationships (Fig. 11) and condition of static lever equilibrium, it is possible to calculate interface load capacity, F_r, and interface compliance, ξ_1, at point O_1:

$$F_r = (F_o \cdot y_o - M_t) / e \tag{2}$$

$$\xi_1 \approx e \cdot \xi / y_o \tag{3}$$

Table 2 Regression equations and correlation coefficients, R, obtained by statistical analysis of experimental results

Indenter	Regression equation	R
Cone α=60°	$F_r = -8022.812 \cdot \xi_1 + 0.023212 \cdot F_{ind} - 10750.3 \cdot \xi_1^{0.806709} + 95.13135 \cdot (\xi_1 \cdot F_{ind})^{1/2}$	0.962
Cone α=90°	$F_r = -4202.98 \cdot \xi_1 + 0.054950 \cdot F_{ind} - 4.38245 \cdot \xi_1^{-0.485342} + 49.56835 \cdot (\xi_1 \cdot F_{ind})^{1/2}$	0.913
Cone α=120°	$F_r = 518.3731 \cdot \xi_1 + 0.039458 \cdot F_{ind} - 1.02334 \cdot \xi_1^{-0.592816} + 37.25787 \cdot (\xi_1 \cdot F_{ind})^{1/2}$	0.974
Speherical R=5	$F_r = -213.146 \cdot \xi_1 + 0.034558 \cdot F_{ind} - 3.63106 \cdot \xi_1^{-0.451858} + 34.39125 \cdot (\xi_1 \cdot F_{ind})^{1/2}$	0.888

Fig. 12 Photo images of the device for measuring interface load capacity and compliance

where: F_r – interface load capacity, F_o - interface load at point A, M_t - friction torque of tapered roller bearing, e - offset of indenting point relative to lever axis of rotation, y_o - offset of the point of application of force F_o, to the axis of rotation, ξ_1 - compliance of test insert/indenter interface at point O_1, ξ - displacement of test lever in the direction of X axis at point A which represents point of application of force F_o.

All deformations (deformations of test lever, and other levers of the measuring system, as well as the deformations of indenters) can be disregarded relative to the test insert/indenter interface compliance. It is also important to note the following:

- Measuring device (Fig. 12) is designed to allow application of a set of constant indenting force magnitudes with indenters of predefined geometry. However, it does not allow the setting of depth of indent.
- Measuring device provides accurate guiding for the indenter, below 0.0005mm. Considering that the registered values of compliance do not exceed 0.1mm, this accuracy allows reliable measurements.
- Fulcrums of test lever and other levers in the system are realized as high-precision roller bearings and low friction coefficient.
- Tapered roller bearing which is mounted on the test lever is of high quality and features low friction coefficient. To calculate the friction torque for this bearing, experimental data obtained from manufacturer were used.

4. Experimental results

Experimental investigations were conducted on test inserts of annealed steel C 45 E, with tensile strength of 710MPa and 208HB hardness. Chemical composition of steel was following: 0.44% C, 0.18% Si, 0.27% Mn, 0.011% Si, and <0.010% P. Test inserts were of following dimensions: 25mm x 30mm x 50mm. In the experiments, the role of test inserts was to represent workpiece.

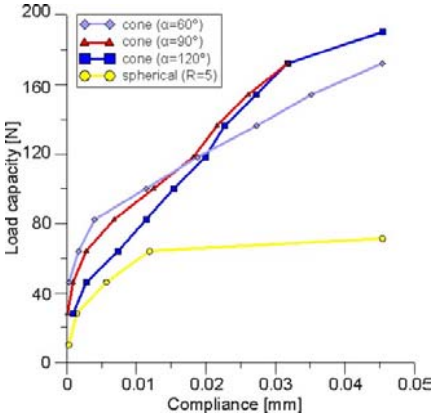

Fig. 13 Dependence of interface load capacity, F_r, on interface compliance, ξ_1, for indenting force of F_{ind}=400N using various indenter geometries

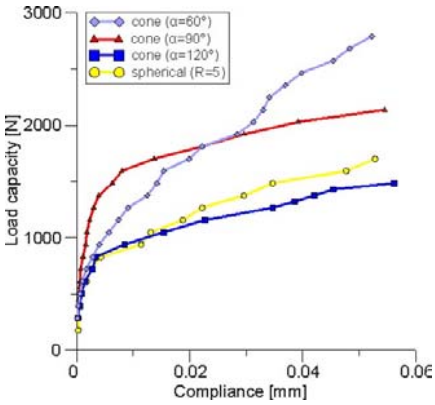

Fig. 14 Dependence of interface load capacity, F_r, on interface compliance, ξ_1, for indenting force of F_{ind}=13000N using various indenter geometries

The indenters were made of hardened tool steel, HS 18-0-1, with 64HRC hardness, and following chemical composition: 0.8% C, 0.5% Si, 0.04% P, 0.03% S, 4.2% Cr, 1.1% V, 18.5% W. Indenters were used in experiments to replace fixture clamping elements. Surface roughness of test inserts/indenters interface was R_a=0.8μm.

Statistical analysis of numerous experimental results yielded regression equations of the surfaces which describe dependence of interface load capacity, F_r, on indenting force magnitude, F_{ind}, and interface compliance, ξ_1, for various indenter geometries (i.e., clamping element geometries). The obtained regression equations and their corresponding coefficients of correlation, R, are presented in Table 2.

Figs. 13 and 14 show dependence of interface load capacity, F_r, on interface compliance, ξ_1, in the case of F_{ind} =400N and F_{ind} =13000N, using various indenter geometries. Shown in Fig. 15 is a

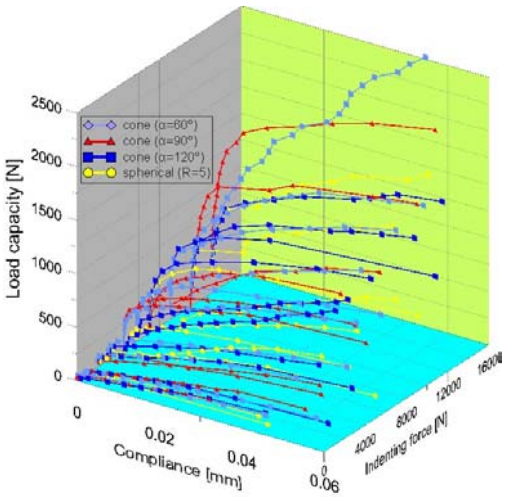

Fig. 15 3D diagram of dependence of interface load capacity, F_r, on interface compliance, ξ_1, indenting force, F_{ind}, and indenter geometry

3D diagram of dependence of interface load capacity, F_r, on interface compliance, ξ_1, indenting force, F_{ind}, and indenter geometry.

Based on the diagram in Fig. 13 one concludes that, in the domain of lower indenting forces, the cone-tip indenters, throughout the entire range of compliances, exhibit significant advantages compared to spherical-tip indenter, which mostly complies with the results of FEM analysis (Fig. 8). Moreover, based on Fig. 14 it can be concluded that α=60° and α=90° indenters, for high loads and within the entire range of compliances, have significantly higher load capacity compared to α=120° and R=5, which also agrees with the results of FEM analysis (Fig. 9). Superior load capacity of cone-tip indenters is basically present within the entire range of simulated indenting forces, which is illustrated by the numerous load capacity curves in Fig. 15.

5. Discussion

Numerical and experimental results indicate that interface load capacity and compliance are a complex matter, regardless of whether the loads are transferred by friction or indenting force. It is very difficult to define a general analytical model which could reliably predict the dependence of interface load capacity as a function of compliance in a wider load interval and for different interface macrogeometries. The stress/strain field distribution for this complex process is performed by Simufact Forming v9 software. The results thus obtained are comparable to experimental ones. The results of numerical analyses and experimental investigations indicate the significant influence of interface macrogeometry on its load capacity and compliance. Based on experimental investigation, it is possible to conclude that, given the same interface compliance, cone-tip indenters provide higher interface load capacities compared to spherical-tip indenter, which transfers the load exclusively by friction. This is especially true in the case of α=60° and α=90° indenters (Figs. 8 and 9). According to

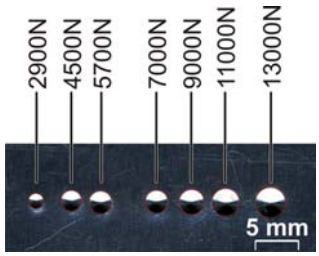

Fig. 16 Imprint marks left by α=120° indenter at various indenting forces

experimental results, in the domain of lower loads (Fig. 13), relative to spherical-tip indenter, all cone-tip indenters exhibit significant advantage considering their load capacity and interface compliance. The numerical analyses also back this claim. Compared to spherical-tip indenter at higher loads (Fig. 14), α=90° and, especially, α=60° indenter, have significant advantage considering their load capacity and interface compliance. This comes to prominence in cases when machining with high cutting forces. Compared to spherical-tip indenter, (R=5), cone-tip indenters in many cases have higher load capacity and interface compliance within the entire interval of analyzed indenting forces.

During indenting process, the indenter which simulates fixture clamping element, penetrates the test insert which simulates workpiece. Since, regardless of their geometry, the indenters have the hardness of 64 HRC, their deformations can be disregarded compared to workpiece deformation. Shown in Fig. 16 are some of the imprint marks created by α=120° indenter at various loads. It should be noted that the imprint marks were measured after disassembly, which made it impossible to establish the share of elastic deformations, i.e., the reduction of imprint diameter after cessation of indenting force. With this in mind, it is possible that some measuring errors were present. However, test inserts were made of annealed steel and during indenting suffered a significant share of plastic deformations. Based on this fact, and the distinctive trend of change of interface load capacity with the change of contact surface macrogeometry, it is supposed that the share of reversible, elastic deformations is small compared to plastic deformation and the measuring error can be disregarded.

Based on the imprint marks and indenter geometry (cone angle, or sphere radius) indentation volumes in test inserts were calculated, as shown in Fig. 17 for all tested indenters. Based on the diagram in Fig. 17 it is evident that the indented volume increases as the indenter tip angle decreases. This is especially true for α=60° indenter at higher loads, i.e., indenting forces. With this in mind, there is a general conclusion that there is a correlation between the indented volume and load capacity, i.e., interface compliance.

One of the key problems in numerical simulation (FEM analysis) was to define the change of friction coefficient as the function of stress at indenter/test insert interface (contact surface), for various indenter geometries. It is well known that friction coefficient, among other parameters, depends on the magnitude of normal stresses which have various distributions for different indenter geometries and cannot be precisely quantified experimentally. For the purpose of numerical simulations, friction

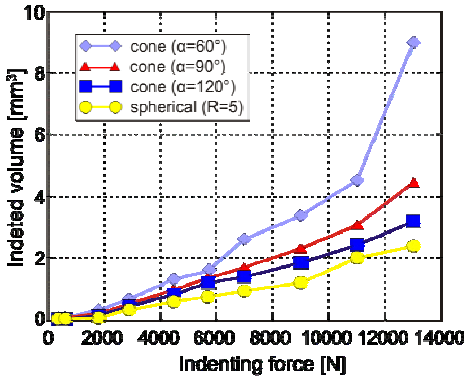

Fig. 17 Dependence of indentation volume on indenting force for various indenter geometries

coefficient was set as a constant value, μ=0.15. This value was determined by tribometric measurement, using Block on Disc tribometer, and represents average value of static friction coefficient for indenter/test insert materials. Considering previous discussion, it is highly probable that the existing differences between experimental and numerical results can be largely attributed to unavoidable approximations.

Voluminous results obtained by FEM analysis and experimentally were statistically analyzed, while the resulting regression surfaces are analytically and graphically represented in Tables 1 and 2, and Fig. 18, respectively. Regression equations are characterized by high coefficients of correlation (R=0.888-0.991) and the trends of change of interface load capacity as the function of interface compliance and indenter geometry. There is a significant compliance between experimental and simulation results considering the ranking of indenter geometry based on load capacity.

The question of quantification of load capacity and interface compliance effects in real conditions, under dynamic machining forces, remains open. The authors maintain that there are numerous facts that speak in favour of the proposed workpiece clamping method and its ability to withstand longer exposure to dynamic forces. Firstly, it should be noted that manufacturers of modular fixtures (Halder, Bluco, Kipp, Norelem, etc.) already have in offer some locating elements which are exposed to similar dynamic loads and their principle of operation is also based on indenting sharp tips into workpiece. Such locating elements have for quite some time been used for machining of castings and forgings. Critical issues regarding the clamping method proposed in this paper are the dynamic factors which can lead to tip wear and blunting, plastic deformations and increased clamping element/workpiece interface compliance. Three most influential factors are: relative speed, i.e., velocity of workpiece oscillation relative to indenter (clamping element), intensity of indenter wear, the magnitude and law of change of the dynamic tangential load of indenter/workpiece interface. If the magnitude of clamping force is sufficient to provide the required initial interface load capacity, then it is certain that the workpiece velocity of oscillations relative to indenter shall be kept low. This conclusion is based on low oscillation amplitudes[34,35] and oscilation frequencies of the dynamic component of the cutting

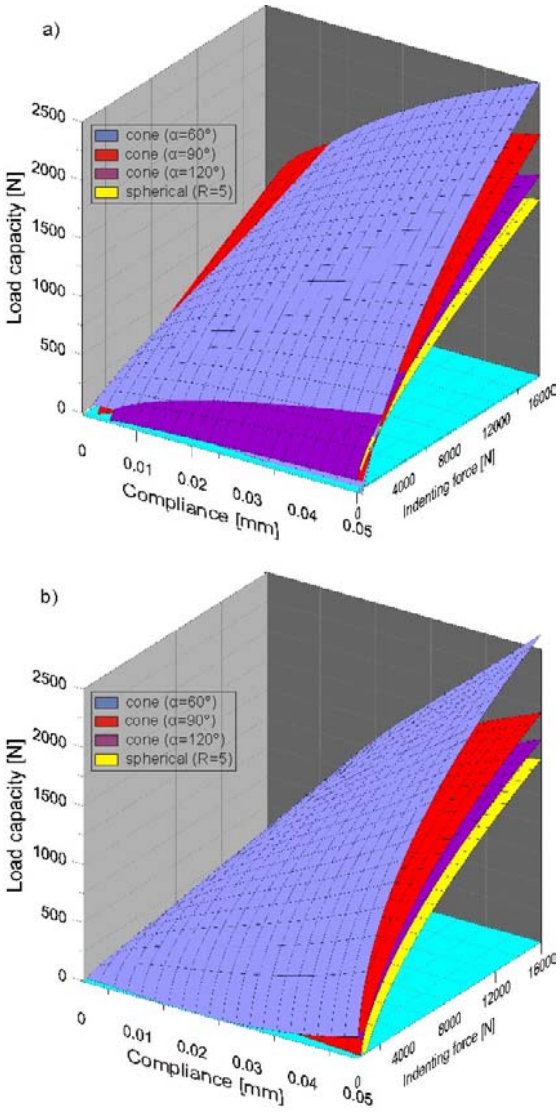

Fig. 18 Comparative 3D diagrams of interface load capacities, F_r, (a) obtained by FEM analysis, and (b) obtained experimentally

force.

It is well known that the relative velocity of contact pair elements has a dominant influence on wear. Moreover, the wear increases with velocity. Bearing in mind that indenters can be made of quality tool materials (e.g., coated hard metals) which are resistant to wear and plastic deformation even at cutting speeds the magnitude of hundreds of m/min and high loads, then it is right to suppose that the proposed clamping system can be successfully used in real conditions under dynamic loads caused by cutting forces. More precisely, a number of modern tool inserts feature cutting wedge angles less than 90° and very sharp cutting edges which remain so through long intervals of intensive machining. These inserts are made of high quality tool materials, with coatings, and can operate under conditions (high cutting speeds and high dynamic loads) which are critical from the aspect of tool wear and tool plastic deformations. With this in mind, it is not quite possible to foresee all the advantages of the proposed clamping method in comparison to conventional clamping with clamp screws or strap clamps. However, the results obtained with structural analysis and

this brief review of process dynamics, provide sufficient motivation for the continuation of investigation of the behavior of the proposed clamping method under real dynamic loads which emerge during machining process.

6. Conclusions

Based on the previous discussion, following conclusions can be drawn:

- Simulated in this paper was the process of clamping with a spherical-tip clamping screw while the load capacity and interface compliance were monitored at while the force acted normally to the direction of clamping force. It was established that this popular clamping method has significantly lower load capacity compared to interfaces which were realized by indenting cone-tip indenters (simulating clamping element) into test-inserts (simulating workpiece).
- FEM analysis and experiment yielded similar results. They both showed that smaller cone tip angles result in significant increase of interface load capacity. The obtained results also indicate that within the entire range of simulated clamping force, cone-tip indenters exhibit superiority compared to spherical-tip indenter.
- Smaller cone tip angles produce larger indented volumes, which correspond to higher load capacities and lower compliances. It is obvious that larger indented volumes correspond, on average, to smaller compression stresses at indenter/test insert interface, which results in lower interface compliance when applying external force in the direction normal to indenter axis. In other words, larger indented volumes correspond to higher interface load capacities.
- Practical applicability of the proposed clamping method lies in the domain of workpieces which, considering their function and aesthetic features, can tolerate local deformations in narrow zones. This is most often the case with castings and forgings of various geometries.
- In order to meet the requirements of the proposed clamping method, the clamping elements (clamp screws or strap clamps) should be fitted with hard metal or tool steel inserts, which is feasible operation from the technical and economic point of view.
- Considering the sophistication of today's tool materials and small velocity of workpiece oscillation relative to fixture clamping elements in a well designed fixture, it is realistic to expect good performance of the proposed clamping method in real machining conditions. Moreover, based on previous discussion, low wear and insignificant plastic deformations of indenters, i.e., clamping elements, are also to expect.

Future investigations should be aimed towards two goals. The first goal is optimization of the proposed clamping elements design. The second is optimization of methods which allow assessment of application effects of the proposed clamping method in modern manufacturing conditions, under pronounced dynamic loads.

REFERENCES

1. Chun, S. H. and Ko, T. J., "Study on the response surface model of machining error in internal lathe boring," Int. J. Precis. Eng. Manuf., Vol. 12, No. 2, pp. 177-182, 2011.
2. Vukelic, D., Zuperl, U., and Hodolic, J., "Complex system for fixture selection, modification, and design," Int. J. Adv. Manuf. Technol., Vol. 45, No. 7, pp. 731-748, 2009.
3. Munawar, M., Chen, J., and Mufti, N., "Investigation of cutting parameters effect for minimization of sur face roughness in internal turning," Int. J. Precis. Eng. Manuf., Vol. 12, No. 1, pp. 121-127, 2011.
4. Vukelic, D., Ostojic, G., Stankovski, S., Lazarevic, M., Tadic, B., Hodolic, J., and Simeunovic, N., "Machining fixture assembly/disassembly in RFID environment," Assem. Autom., Vol. 31, No. 1, pp. 62-68, 2011.
5. Bi, Z. M. and Zhang, W. J., "Flexible fixture design and automation: Review, issues and future directions," Int. J. Prod. Res., Vol. 39, No. 13, pp. 2867-2894, 2001.
6. Wan, X. J., Hua, L., Wang, X. F., Peng, Q. Z., and Qin, X. P., "An error control approach to tool path adjustment conforming to the deformation of thin-walled workpiece," Int. J. Mach. Tools Manuf., Vol. 51, No. 3, pp. 221-229, 2011.
7. Amaral, N., Rencis, J. J., and Rong, Y., "Development of a finite element analysis tool for fixture design integrity verification and optimisation," Int. J. Adv. Manuf. Technol., Vol. 25, No. 5, pp. 409-419, 2005.
8. Asante, J. N., "A combined contact elasticity and finite element-based model for contact load and pressure distribution calculation in a frictional workpiece-fixture system," Int. J. Adv. Manuf. Technol., Vol. 39, No. 5-6, pp. 578-588, 2008.
9. Chen, W., Ni, L., and Xue, J., "Deformation control through fixture layout design and clamping force optimization," Int. J. Adv. Manuf. Technol., Vol. 38, No. 9, pp. 860-867, 2008.
10. De Meter, E. C., Xie, W., Choudhuri, S., Vallapuzha, S., and Trethewey, M. W., "A model to predict minimum required clamp pre-loads in light of fixture–workpiece compliance," Int. J. Mach. Tools Manuf., Vol. 41, No. 7, pp. 1031-1054, 2001.
11. Hamedi, M., "Intelligent fixture design through a hybrid system of artificial neural network and genetic algorithm," Artif. Intell. Rev., Vol. 23, No. 3, pp. 295-311, 2005.
12. Hockenberger, M. J. and DeMeter, E. C., "The application of meta functions to the quasi-static analysis of workpiece displacement within a machining fixture," J. Manuf. Sci. Eng.-Trans. ASME., Vol. 118, No. 3, pp. 325-331, 1996.
13. Huang, Y. and Wang, L., "Realizing high accuracy machining by applying optimal clamping forces," Int. J. Comput. Appl. Technol., Vol. 19, No. 2, pp. 107-118, 2004.
14. Kashyap, S. and DeVries, W. R., "Finite element analysis and optimization in fixture design," Struct. Optim., Vol. 18, No. 2-3,

pp. 193-201, 1999.

15. Kaya, N., "Machining fixture locating and clamping position optimization using genetic algorithms," Comput. Ind., Vol. 57, No. 2, pp. 112-120, 2006.
16. Krishnakumar, K. and Melkote, S. N., "Machining fixture layout optimization using the genetic algorithm," Int. J. Mach. Tools Manuf., Vol. 40, No. 4, pp. 579-598, 2000.
17. Kulankara, K., Satyanarayana, S., and Melkote, S. N., "Iterative fixture layout and clamping force optimization using the genetic algorithm," J. Manuf. Sci. Eng.-Trans. ASME., Vol. 124, No. 1, pp. 119-125, 2002.
18. Liao, Y. J., Hu, S. J., and Stephenson, D. A., "Fixture layout optimization considering workpiece-fixture contact interaction: simulation results," Trans. NAMRI/SME, Vol. 26, pp. 341-346, 1998.
19. Liu, S.-G., Zheng, L., Zhang, Z.-H., Li, Z.-Z., and Liu, D.-C., "Optimization of the number and positions of fixture locators in the peripheral milling of a low-rigidity workpiece," Int. J. Adv. Manuf. Technol., Vol. 33, No. 7, pp. 668-676, 2007.
20. Lu, Y., Qin, G., and Li, M., "A Cellular Genetic Algorithm Based Optimization of Clamping Forces for Fixture Design," Adv. Sci. Lett., Vol. 4, No. 6-7, pp. 2342-2346, 2011.
21. Prabhaharan, G., Padmanaban, K. P., and Krishnakumar, R., "Machining fixture layout optimization using FEM and evolutionary techniques," Int. J. Adv. Manuf. Technol., Vol. 32, No. 11-12, pp. 1090-1103, 2007.
22. Padmanaban, K. P. and Prabhaharan, G., "Dynamic analysis on optimal placement of fixturing elements using evolutionary techniques," Int. J. Prod. Res., Vol. 46, No. 15, pp. 4177-4214, 2008.
23. Padmanaban, K. P., Arulshri, K. P., and Prabhakaran, G., "Machining fixture layout design using ant colony algorithm based continuous optimization method," Int. J. Adv. Manuf. Technol., Vol. 45. No. 9-10, pp. 922-934, 2009.
24. Ratchev, S., Phuah, K., and Liu, S., "FEA-based methodology for the prediction of part-fixture behaviour and its applications," J. Mater. Process. Technol., Vol. 191, No. 1-3, pp. 260-264, 2007.
25. Sánchez, H., Estrems, M., and Faura, F., "Fixturing analysis methods for calculating the contact load distribution and the valid clamping regions in machining processes," Int. J. Adv. Manuf. Technol., Vol. 29, No. 5, pp. 426-435, 2006.
26. Satyanarayana, S. and Melkote, S. N., "Finite element modeling of fixture–workpiece contacts: single contact modeling and experimental verification," Int. J. Mach. Tools Manuf., Vol. 44, No. 9, pp. 903-913, 2004.
27. Siebenaler, S. P. and Melkote, S. N., "Prediction of workpiece deformation in a fixture system using the finite element method," Int. J. Mach. Tools Manuf., Vol. 46, No. 1, pp. 51-58, 2006.
28. Tan, E. Y. T., Kumar, A. S., Fuh, J. Y. H., and Nee, A. Y. C., "Modeling, analysis, and verification of optimal fixturing design," IEEE Trans. Autom. Sci. Eng., Vol. 1, No. 2, pp. 121-132, 2004.
29. Vishnupriyan, S., Majumder, M. C., and Ramachandran, K. P., "Optimal fixture parameters considering locator errors," Int. J. Prod. Res., Vol. 49, No. 21, pp. 6343-6361, 2011.
30. Wang, Y., Chen, X., Gindy, N., and Xie, J., "Elastic deformation of a fixture and turbine blades system based on finite element analysis," Int. J. Adv. Manuf. Technol., Vol. 36, No. 3-4, pp. 296-304, 2008.
31. Wang, Y., Xie, J., Wang, Z., and Gindy, N., "A parametric FEA system for fixturing of thin-walled cylindrical components," J. Mater. Process. Technol., Vol. 205, No. 1-3, pp. 338-346, 2008.
32. Xiong, C. H., Wang, M. Y., and Xiong, Y. L., "On Clamping Planning in Workpiece-Fixture Systems," IEEE Trans. Autom. Sci. Eng., Vol. 5, No. 3, pp. 407-419, 2008.
33. Zuperl, U., Cus, F., and Vukelic, D., "Variable clamping force control for an inteligent fixturing," J. Prod. Eng., Vol. 14, No. 1, pp. 19-22, 2011.
34. Hurtado, J. F. and Melkote, S. N., "Workpiece-fixture static friction under dynamic loading," Wear, Vol. 231, No. 1, pp. 139-152, 1999.
35. Liao, Y. G. and Hu, S. J., "An Integrated Model of a Fixture–Workpiece System for Surface Quality Prediction," Int. J. Adv. Manuf. Technol., Vol. 17, No. 11, pp. 810-818, 2001.